The cooling of the pressing device in the glass industry

Petr SALAČ[1*] and Michal STARÝ[2]
[1]Faculty of Science, Humanities and Education, Technical University of Liberec, Studentská 2, 46117 Liberec, Czech Republic
[2]Faculty of Mechanical Engineering, Technical University of Liberec, Studentská 2, 46117 Liberec, Czech Republic
michal.stary@tul.cz

ABSTRACT
In this article we investigate the problem of shape optimization of the cooling cavity of the plunger used in the forming process in the glass industry. A rotationally symmetrical system consisting of the mould, the glass piece, the plunger and the plunger cavity is considered. The state problem is given as a stationary head conduction equation. The system has a given heat source which represents the glass piece and is cooled by flowing water inside the plunger cavity and by the environment of the mould on the outside. The design variable is taken to be the shape of inner surface of the plunger cavity. According to the results of the verification experiments, it is possible to claim that the numerical optimization that was achieved brought about a significant improvement. Further an unsteady periodic experiment representing the cyclical movement in a realistic working mode was performed to examine the effect of replacing it with the static model.

1. INTRODUCTION

There are two main problems during glass pressing on the surface of a moulded piece. On one hand, if the surface of the plunger is too hot at the moment of separation of the moulded piece and the plunger, then the glass melt adheres to the device and results in the deformation of the moulded piece. Conversely, if the surface of the plunger is too cold, then small fire cracks appear on the surface of the moulded piece, which means poorer quality of production. For these reasons, it is desirable to achieve a constant distribution of temperature across the surface of the moulding device when the plunger separates from the moulded piece.

The main goal of optimization is to control the temperature distribution on the outer surface of the plunger during the pressing cycle in the production of glass vases. Firstly, the molten glass is poured into the mould and then the plunger descends from above, in order to press the vase, and stays about 10 seconds in the lowered position. Then the plunger leaves the vase. From the technological point of view we need the prescribed constant temperature across the outward surface of the plunger at the moment of separation.

We are going to change the cavity shape to change the distance between the glass and the cooling water in the first step of optimization and to change the shape of the regulation current body to control the velocity of the water. Both result in the ability to control the local intensity of cooling at the outward surface of the plunger.

*Corresponding author. E-mail: petr.salac@tul.cz

2. MATHEMATICAL FORMULATION

The mathematical model is a strong idealization of a non-stationary periodic problem of heat conduction. Here, we study the problem of stationary conduction of heat for mean values of this periodic process with cooling by stationary flowing water.

We consider the union of the four regions $\Omega = \Omega_{Mo} \cup \Omega_{Gl} \cup \Omega_{Pl} \cup \Omega_{Ca}$ that represents the mould, the glass piece, the plunger and the cooling cavity of the plunger. In the cavity we assume the potential water flow described by the Neumann problem

$$\Delta\Phi = 0 \quad \text{in} \quad \Omega_{Ca}, \tag{1}$$

$$\frac{\partial\phi}{\partial n} = g \quad \text{on} \quad \partial\Omega_{Ca}, \tag{2}$$

where $g \epsilon L^2(\partial\Omega_{Ca})$ represents the normal component of the water flow velocity at the entrance to and the exit from the plunger cavity in the form

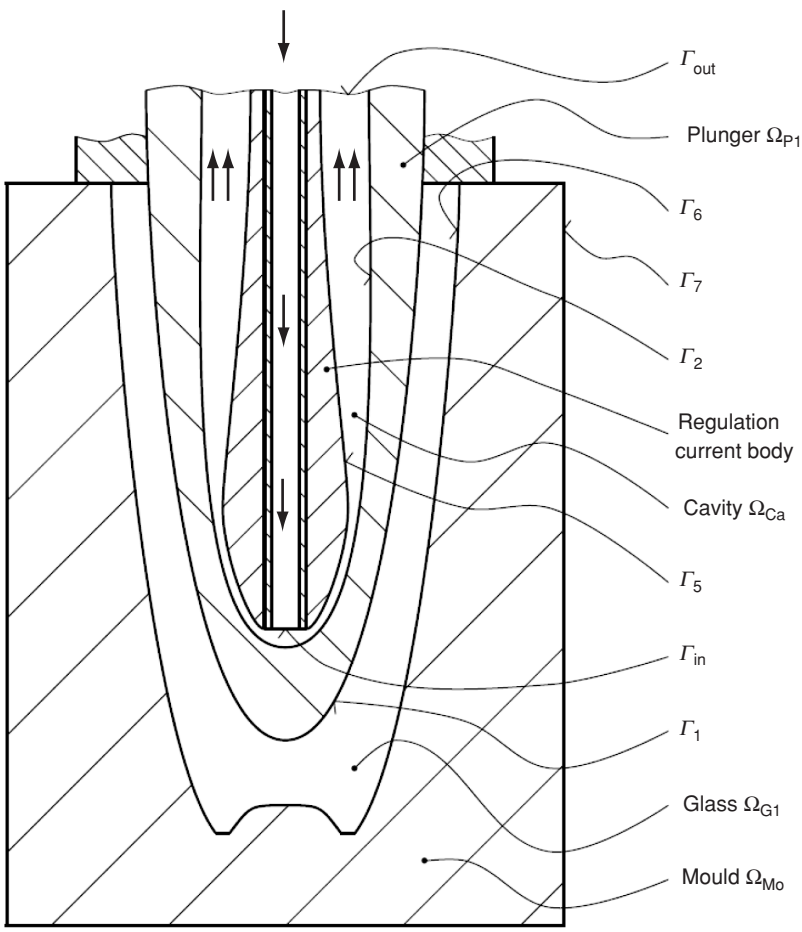

Figure 1 Scheme of the system the mould, the glass piece, the plunger, the plunger cavity and the regulation current body.

$$g = \begin{cases} 0 & \text{on } \Gamma_2 \cup \Gamma_5, \\ h_{velo}^{in} & \text{on } \Gamma_{in}, \\ h_{velo}^{out} & \text{on } \Gamma_{out}, \end{cases} \tag{3}$$

h_{velo}^{in} (m/s) represents the normal velocity at the entrance Γ_{in} and h_{velo}^{out} (m/s) is the normal velocity at the exit Γ_{out}. The flowing water has velocity $u = (u_1, u_2, u_3)$ (m/s) given as

$$u = g\,\mathrm{grad}\Phi \quad \text{in } \Omega_{Ca}. \tag{4}$$

We put $u = 0$ in $\Omega_{Mo} \cup \Omega_{Gl} \cup \Omega_{Pl}$. We substitute the velocity vector u to the energy equation

$$c_v \mathrm{grad}\,\vartheta . u - \frac{k}{\varrho}\Delta\vartheta = q, \tag{5}$$

where c_v (J/m^3) is the specific heat capacity per unit volume, ϑ (K) is the absolute temperature, k (W/mK) is the coefficient of thermal conductivity and q (W/m^3) is the density of heat sources. We consider $q = 0$ in $\Omega_{Mo} \cup \Omega_{Pl} \cup \Omega_{Ca}$. This means that the problem includes both the pure conduction of heat in the regions $\Omega_{Mo} \cup \Omega_{Gl} \cup \Omega_{Pl}$ and the combination of heat convection with conduction of heat in the region Ω_{Ca}.

We assume the following boundary and transfer conditions:

In the entrance the cooling water has a constant temperature of 288 ^oK, thus

$$\vartheta\big|_{\Gamma_{in}} = 288 \;\; on\; \Gamma_{in}. \tag{6}$$

The output distribution of the temperature is given by the function $h_{out}^e \in C(\Gamma_{out})$ thus

$$\vartheta\Big|_{\Gamma_{out}} = h_{out}^e \quad \text{on } \Gamma_{out}. \tag{7}$$

We assume that the regulation current body is made from insulating material, thus

$$\frac{\partial\vartheta}{\partial n} = 0 \quad \text{on } \Gamma_5. \tag{8}$$

The heat-transfer through Γ_2 is modeled as a boundary condition for contact of two bodies where "the body" representing water includes both the convective and the conductive terms (see [3]), thus

$$-k_{Pl}\frac{\partial\vartheta}{\partial n_{Pl}} = -k_{Ca}\frac{\partial\vartheta}{\partial n_{Ca}} \;\text{ on }\; \Gamma_2, \tag{9}$$

where ∂n_{Pl} and ∂n_{Ca} denote the derivative according to the outward normal with respect to the region Ω_{Pl} and Ω_{Ca} respectively. The coefficients k_{Pl} and k_{Ca} are the thermal conductivity of the plunger and water respectively.

The heat-transfer through the boundary Γ_7 is modeled as a boundary condition of the third kind for contact between the body and the environment (see [3]), thus

$$-k_{Mo}\frac{\partial \vartheta}{\partial n_{Mo}} = \alpha\left(\vartheta\big|_{\Gamma_7} - \vartheta_{en}\right) \text{ on } \Gamma_7, \tag{10}$$

where ∂n_{Mo} denotes the derivative according to the outward normal with respect to the region Ω_{Mo} and k_{Mo} is the coefficient of the thermal conductivity of the mould, $\alpha > 0$ (W/m^{2}K) denotes the coefficient of heat-transfer between the mould and the environment, $\vartheta\big|_{\Gamma_7}$ the trace of ϑ on the boundary of the region Ω_{Mo} and $\vartheta_{en} > 0$ the temperature of the environment.

We use the transit condition for contact between two bodies, where one of them changes state because of the influence of solidification (see [3]). The heat-transfer through the boundary Γ_1 between Ω_{Gl} and Ω_{Pl}, and through the boundary Γ_6 between Ω_{Gl} and Ω_{Mo} are described as

$$k_{GL}\frac{\partial \vartheta}{\partial n_{Gl}} - k_{Pl}\frac{\partial \vartheta}{\partial n_{Pl}} = \beta_1 \text{ on } \Gamma_1, \tag{11}$$

and

$$k_{Gl}\frac{\partial \vartheta}{\partial n_{Gl}} - k_{Mo}\frac{\partial \vartheta}{\partial n_{Mo}} = \beta_6 \text{ on } \Gamma_6, \tag{12}$$

where ∂n_{Gl} denotes the derivative according to the outward normal with respect to the region Ω_{Gl} and k_{Gl} is the coefficient of thermal conductivity of glass, β_1 and β_6 (J/m^{2}s) denote the flux density of the modified mass of the glass.

The problem (1)–(12) has a unique solution and can be used as the state problem to formulate the problem of the optimal design for the plunger cavity shape (see [3]) and the problem of the optimal design for the regulation current body shape (see [4]). We are looking for such a shape of the boundary Γ_2 and Γ_5, such that the cost functionals

$$\Im^S(\Gamma_2) = \| \vartheta(\Gamma_2)|_{\Gamma_1} - K \|^2_{0.r.\Gamma_1} \tag{13}$$

and

$$\Im^P(\Gamma_5) = \| \vartheta(\Gamma_5)|_{\Gamma_1} - K \|^2_{0,r,\Gamma_1} \tag{14}$$

take the minimum value in the set of admissible design functions.

We denote by $\vartheta(\Gamma_2)\big|_{\Gamma_1}$ and $\vartheta(\Gamma_5)\big|_{\Gamma_1}$ the traces of ϑ derived from the shapes boundary Γ_2 and Γ_5 on the boundary Γ_1 of the region Ω_{Pl} respectively. Further we denote by $\|.\|_{0,\,r,\,\Gamma_1}$ the norm in an appropriate weighted space L^2_r.

3. LABORATORY EXPERIMENTS DESCRIPTION

To verify the numerical results, a series of comparative experiments between a classic and optimized plunger were performed.

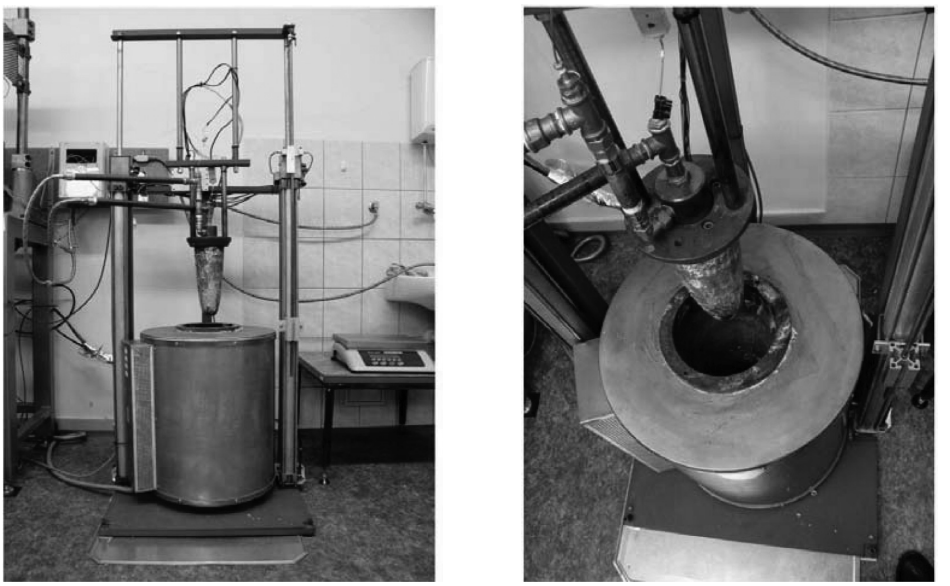

Figure 2 Laboratory workplace.

The main part of the laboratory workplace (see figure 2), that has been created, is a special 5 kW pot-type furnace with an interior of 19 dm^3. A cast-iron melting pot is put in the furnace cavity, in which is melted the desired amount of tin which is the substitute for the glass melt [1, 2, and 7]. Above the furnace is placed a plunger which is held by two parallel pneumatic cylinders.

The plunger, the shape of which is designed in the conventional way, is made in two versions. The first is with a drilled hole (figure 3a) and the second with a shape-optimized cavity (figure 3b). Into the plunger with the drilled hole, a common stainless pipe is inserted as a water inlet. Into the plunger with the shaped cavity, which was designed according to numerical optimization, is inserted a plastic regulation current body from Murpec, the profile of which was also specified by numerical optimization. A special fitting with the fixed cooling device is set into the plunger, which provides the coolant inlet and therefore also the outlet. The water temperature is monitored at the plunger cavity input (thermocouple no. 13), at the very end of the pipe or the regulation current body, and also at the plunger output, at the fitting to be precise (thermocouple no. 14). Both versions are equipped with 12 sheathed K-type thermocouples which are distributed across the surface at different places (see figure 3) and at relevant depths of the plungers in order to monitor the temperature field. The main thermocouples, numbers 1, 4, 7 and 10, which are found close to the surface (5 mm under) are for optimization. To monitor the temperature development through the entire cross section of the tool thermocouples numbers 2 and 5 at a depth of 10 mm are placed, then 3, 6, 8 and 11 at a distance of 15 mm and a thermocouples 9 and 12 at a distance of 25 mm from the surface.

The experiments were conducted in two stages. The first stage of the experiment is carried out as a static case where the plunged plunger is permanently submerged. This corresponds to the numerical optimization model and guarantees clear (fixed) conditions and, due to lower temperatures, the correct functioning of the regulation current body, because in this case all the water in the whole system is sure to be in a liquid state. In the

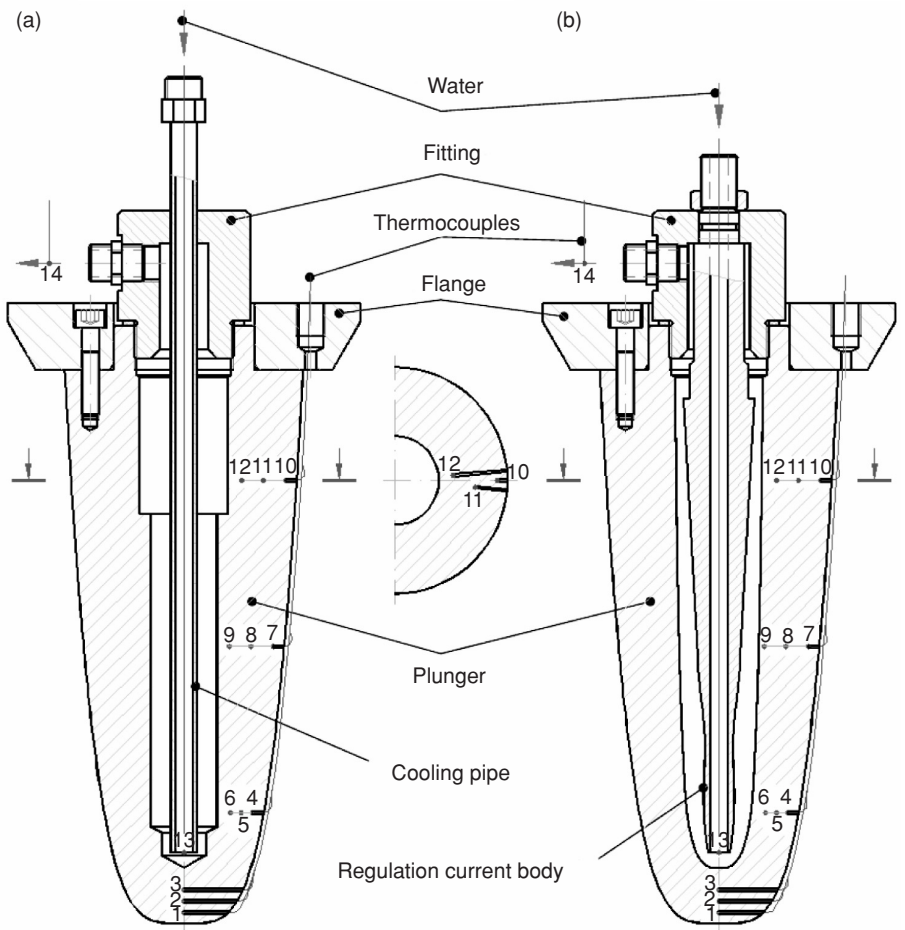

Figure 3 Cross-section of plungers with inbuilt cooling system and thermocouples. (a) Plunger I: classic plunger with a drilled hole and a standard cooling pipe. (b) Plunger II: plunger with a shape-optimized cavity and a flow control body.

second stage of the experiment the plunger works in a cyclic movement as in a realistic working mode. In this case, it means at higher temperature, it is necessary to prevent local boiling and a subsequent change of state from water to steam.

Before starting the experiments in the first stage the workplace must be prepared which means submerging the correct plunger into the tin bath and then letting the whole system cool down. Starting the experiments consists of regulating the flow of the cooling water, specifically at 0.5 l/min, and next the furnace is turned on at full power.

The preparatory work of the second stage of the experiments consists of tin melting where the furnace temperature is set to 600 °C, the plunger preheated to 50–70 °C and activating the water cooling where the flow is set to 1 l/min. The flow is set to prevent the water from boiling. The experiment starts by submerging the plunger into the tin bath. The plunger working cycle takes 28 s and is shown in figure 4.

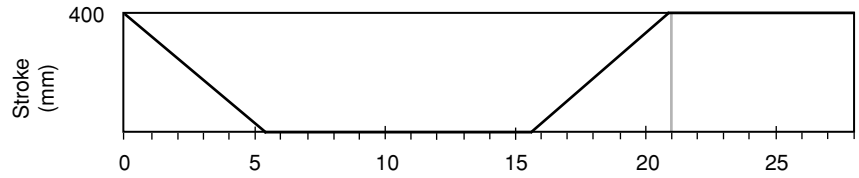

Figure 4 Working mode of the plungers during the second stage – cyclic mode.

4. EXPERIMENTAL RESULTS OVERVIEW

4.1. FIRST EXPERIMENTAL STAGE– STATIC CASE AS IN THE NUMERICAL OPTIMIZATION MODEL

The measured time curve of all monitored mean temperatures for the static case of experiments is shown in figure 5 and figure 6. Although the data are recorded and processed at intervals of 0.1 of a second, in the graphs they are presented at intervals of 5 minutes for the sake of clarity. From the results it is possible to see that the final temperature is reached after about 2.5 to 3 hours from the start of the experiment. By comparing both graphs we can see the difference in the temperature of water (thermocouple no. 13) entering the plunger compared to water exiting the cooling object. It is due to the fact that the presented values do not exactly reflect the inlet water temperature, which was about 10 to 14 °C during the experiment, but rather the temperature at the specific point where the inlet water and current (warmed) water in the plunger may happen to mix. The temperature difference is caused especially by the type of flow and water quantity in the given area of each of the plungers. With regard to the optimization criterion, which is a uniform temperature of the plunger surface; although the main measurements are considered to be on the plunger surface, in fact they are 5 mm under the surface. These temperatures are marked in bold (full points) in the

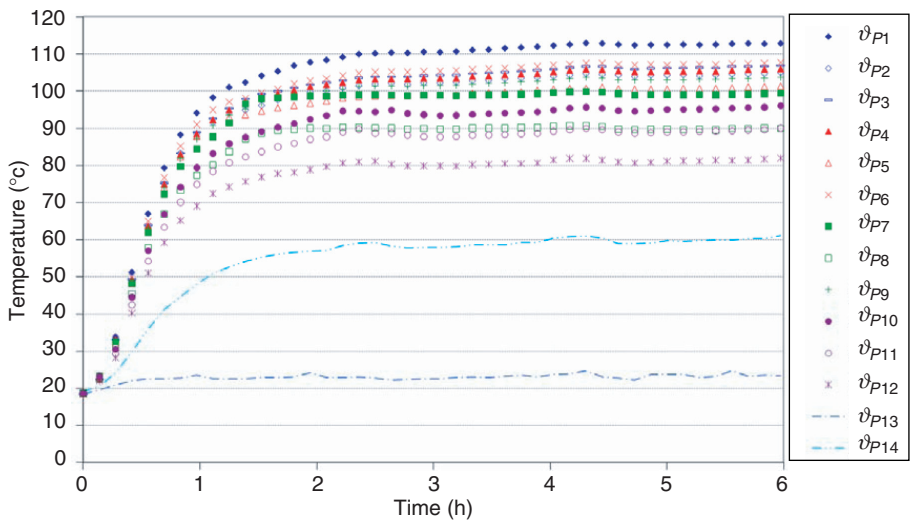

Figure 5 Time curve of all measured temperatures of plunger I in static mode ϑ_{P1} – ϑ_{P12}: temperatures of points in the plunger (figure 3); ϑ_{P13}: temperature of water entering the plunger; ϑ_{P14}: temperature of water exiting the plunger.

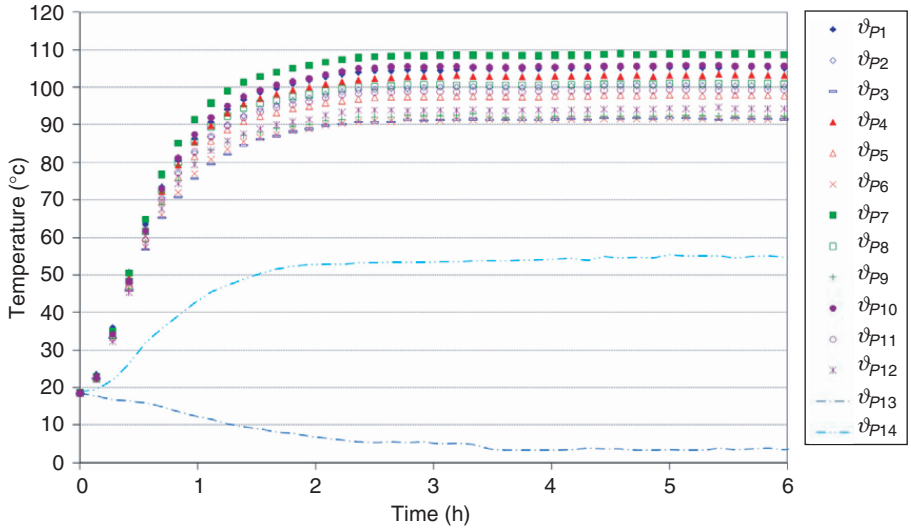

Figure 6 Time curve of all measured temperatures of plunger II in static mode ϑ_{P1} – ϑ_{P12}: temperatures of points in the plunger (figure 3); ϑ_{P13}: temperature of water entering the plunger; ϑ_{P14}: temperature of water exiting the plunger.

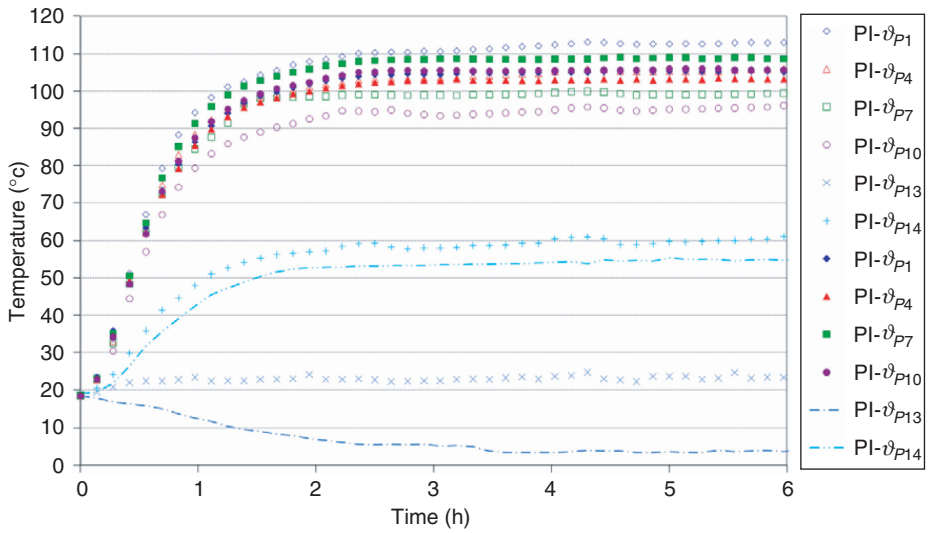

Figure 7 Comparison of surface temperatures of both plungers in static mode PI, II: plunger I, II; $\vartheta_{P1,4,7,10}$: temperatures of relevant points in the plunger (see figure 3); ϑ_{P13}: temperature of water entering the plunger; ϑ_{P14}: temperature of water exiting the plunger.

graphs. For better comparison, the surface temperatures of both plungers are presented in a separate graph, see figure 7.

The results of five measurements of the original plunger construction (Plunger I) and the results of five measurements of the plunger with the optimized cooling cavity and applied

Table 1 Stagnation temperatures for 5 measurements for each plunger.

	Plunger I					**Plunger II**				
Experiment	**1.**	**2.**	**3.**	**4.**	**5.**	**1.**	**2.**	**3.**	**4.**	**5.**
ϑ_{P1}[°C]	113.4	113.3	113.0	112.9	112.5	108.9	105.1	104.7	105.8	101.7
ϑ_{P4}[°C]	104.3	105.8	106.8	106.1	106.2	105.0	102.2	103.1	104.7	100.7
ϑ_{P7} [°C]	101.9	99.3	100.0	98.7	98.2	109.5	107.9	109.3	109.1	107.8
ϑ_{P10} [°C]	96.7	96.2	96.9	95.7	95.0	105.9	105.2	106.6	105.5	104.9
$\Delta_{\max}$ [°C]	**16.7**	**17.1**	**16.1**	**17.2**	**17.5**	**4.5**	**5.7**	**6.2**	**4.4**	**7.1**
$\overline{\vartheta}_i$	100.8	100.1	100.8	99.8	99.3	106.9	105.3	106.5	106.4	104.7
K			100.2					106.0		
$\Im^{Exp}$	**1.21**	**1.50**	**1.51**	**1.67**	**1.89**	**0.30**	**0.33**	**0.38**	**0.24**	**0.60**

regulation current body (Plunger II) are summarized in table 1. Stagnation temperatures after six hours at these points are in the first four lines, the range of measured temperatures are on the fifth line.

The average temperatures computed as a weighted arithmetical mean

$$\overline{\vartheta}_i = \frac{1}{S}(\vartheta_1.S_1 + \vartheta_4.S_4 + \vartheta_7.S_7 + \vartheta_{10}.S_{10}), \tag{15}$$

where the weights are taken as areas of surfaces S_i corresponding to single measurement points P_i, i =1, 4, 7, 10 (see figure 3) are on the sixth line of table 1.

The arithmetical mean of average temperatures from five measurements

$$\mathbf{K} = \frac{\Sigma_{i=1}^{5}\,\overline{\vartheta}_i}{5} \tag{16}$$

is introduced in the seventh line.

The numerical approximations of cost functional (13) and (14) in the form

$$\Im^{Exp} = (\vartheta_{P1} - \mathbf{K})^2.S_1 + (\vartheta_{P4} - \mathbf{K})^2.S_4 + (\vartheta_{P7} - \mathbf{K})^2.S_7 + (\vartheta_{P10} - \mathbf{K})^2.S_{10} \tag{17}$$

are computed. Results are in the last row of the table 1.

The main target of the conducted optimization was to achieve uniform temperature across the entire surface of the plunger.

We are testing the null hypothesis about the correspondence of mean values of the outputs of the cost functional of experimental data obtained from both plungers against the alternative, that the mean value of the outputs of the cost functional on the optimized plunger is statistically significantly less than the mean value of the outputs of the cost functional from the original plunger. We denote μ_1 the mean value of outputs of the cost functional $\Im^{Exp}$ on plunger I and μ_2 the mean value of outputs of $\Im^{Exp}$ on plunger II.

A single tail test about the correspondence of mean values was used, so

$$H_0\text{: } \mu_1 = \mu_2, \tag{18}$$

$$H_1: \mu_1 > \mu_2, \tag{19}$$

where $\mu_1$and μ_2 denote the mean values of outputs of the cost functional on the original plunger and the optimized plunger respectively.

Testing statistic

$$T = \frac{\overline{\Im_1^{Exp}} - \overline{\Im_2^{Exp}}}{\sqrt{\frac{(n_1 - 1).S_1^2 + (n_2 - 1).S_2^2}{n_1 + n_2 - 2}}\sqrt{\frac{1}{n_1} + \frac{1}{n_2}}} = 3.9857, \tag{20}$$

where $\overline{\Im_1^{Exp}}$ and $\overline{\Im_2^{Exp}}$ denote the arithmetical averages of data from sample 1 and sample 2 respectively, n_1 and n_2 the sizes of sample 1 and sample 2 respectively, s_1 and s_2 the standard deviations of data from sample 1 and sample 2 respectively. Quotient

$$\frac{\overline{\mathfrak{I}_2^{Exp}}}{\mathfrak{I}_1^{Exp}} = 0.24 \tag{21}$$

shows the decrease of the point estimate of the mean of the outputs of the cost functional about 76 %.

4.2. SECOND EXPERIMENTAL STAGE – CYCLIC CASE AS IN A REALISTIC WORKING MODE

Measured time curve of all monitored mean temperatures for cyclic mode for plunger I is shown in figure 8 and for plunger II in figure 9.

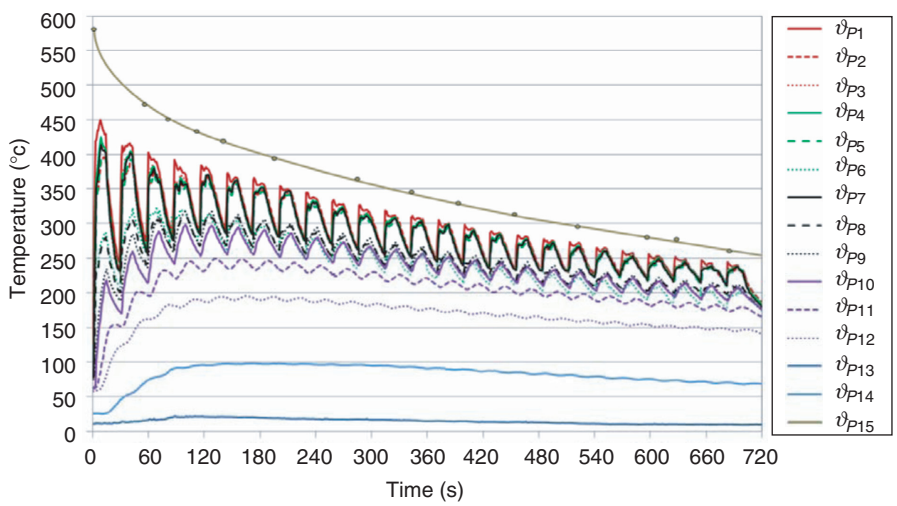

Figure 8 Time curve of all measured temperatures of plunger I in cyclic mode ϑ_{P1} – ϑ_{P12}: temperatures of points in the plunger (figure 3); ϑ_{P13}: temperature of water entering the plunger; ϑ_{P14}: temperature of water exiting the plunger; ϑ_{P15}: temperature trendline of the tin bath.

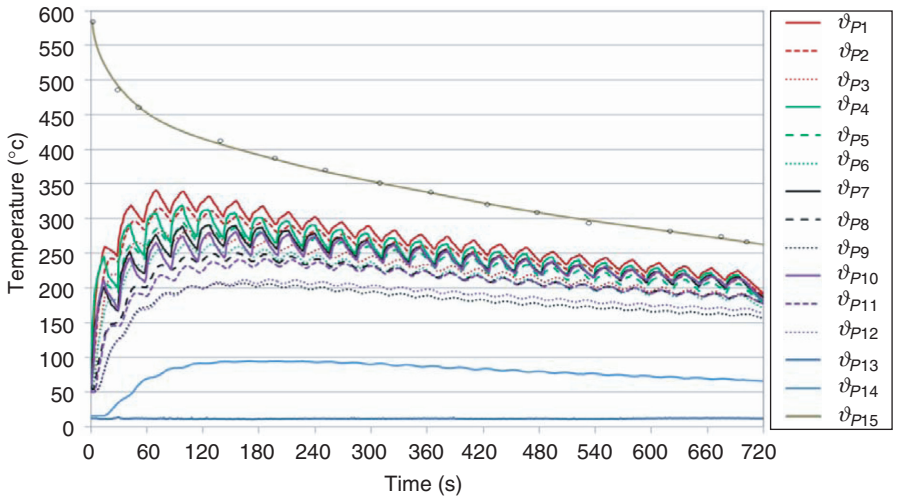

Figure 9 Time curve of all measured temperatures of plunger II in cyclic mode ϑ_{P1} – ϑ_{P12}: temperatures of points in the plunger (figure 3); ϑ_{P13}: temperature of water entering the plunger; ϑ_{P14} temperature of water exiting the plunger; ϑ_{P15}: temperature trendline of the tin bath.

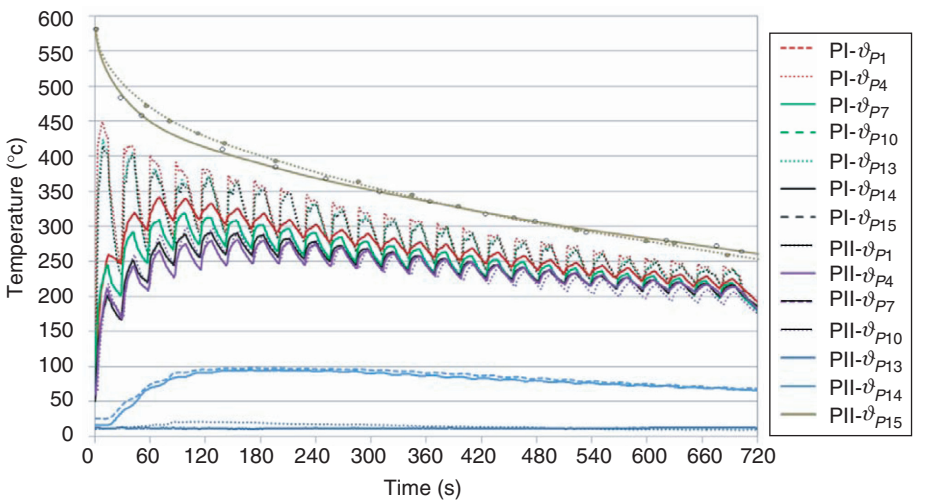

Figure 10 Comparison of surface temperatures of both plungers in cyclic mode PI, II: plunger I, II; $\vartheta_{P1,4,7,10}$: temperatures of relevant points in the plunger (see figure 3); ϑ_{P13}: temperature of water entering the plunger; ϑ_{P14}: temperature of water exiting the plunger; ϑ_{P15}: temperature trendline of the tin bath.

The pseudo-steady state is presented in detail in [5]. For better comparison, the surface temperatures of both plungers are presented in a separate graph, see figure 10. The temperature of the system during the process falls. The duration of the experiment is then limited by the tin freezing point (232 °C) when the tin begins to adhere to the surface of the

plunger. Hence it was usually reached in 25 working cycles. The described situation is given by the limited furnace power and especially by the chosen experimental method, where the same gob (bath) is cooled in contrast to the real working process. Hence the steady state of the working process which is the best for the evaluation was not reached.

5. CONCLUSION

The experimental results of the verification of the numerical optimization confirm a clear trend to uniformity of the surface temperatures of the optimized plunger, which corresponds to the used optimization requirement. From the statistical point of view it is possible to confirm that the results of the static case experiments allow us to reject the null hypothesis, even at significance level $\alpha = 0.005$. That means that we can say with 99.5% probability that the results obtained from the optimized plunger are better than the results obtained from the classic plunger. Specifically, it managed to eliminate the effect of over-cooling of the tip of the plunger as well as improving the temperature in the top half of the plunger. Generally, a 67% reduction of non-uniform temperature on the whole surface of the plunger was achieved, from an average temperature variance of 16.9 °C to 5.6 °C.

From the second stage of the experiments, the results of the plunger in a realistic working mode, it is possible to claim that the uniform thickness of the optimized plunger body, without sharp angles in its shape which could lead to vortex flows, causes more uniform heat sink. Likewise, the lower temperature load which was achieved may contribute to higher durability of the plunger. It is also possible to see that on the optimized plunger steadier (step-less and predictable) temperature curve was achieved.

ACKNOWLEDGEMENT

This research was carried out with the support of the research project MSM 4674788501 financed by the Ministry of Education of the Czech Republic.

REFERENCES

[1] Bertram L. A., Zanner F. J.: Convective Simulation in Metal Solidification, Stability in Convective Flows, ASME, New York (1986), pp. 99–107.

[2] Fukusako S., Seki N.: Fundamental Aspects of Analytical and Numerical Methods on Freezing and Melting Heat Transfer Problems, Annual Review of Numerical Fluid Mechanics and Heat Transfer (1987), vol. 1, pp. 351–402.

[3] Salač P.: Optimal design of the cooling plunger cavity. Appl. Math. 58 (2013), (DOI) 10.1007/s10492-013-0020-8, ISSN 0862-7940, pp. 405-422.

[4] Salač P.: Shape optimization of the regulation current body. Applied Mathematical Modelling. (offered to publish).

[5] Starý M., Salač P.: Verification of Plunger Cooling for Glass Forming in Real Working Mode. EPJ Web of Conferences (2012), Vol. 25, Article No. 01089, source: International conference, Experimental Fluid Mechanics 2011, Jíčín, 22. – 25. 11. 2011, pp. 966–970, ISBN 978-80-7372-784–0.

[6] Šorin S. N.: Sdílení tepla. SNTL, Praha (1968).

[7] Viskanta R.: Heat Transfer During Melting and Solidification of Metals, Journal of Heat Transfer, ASME, New York (1988), vol. 110, iss. 4b, pp. 1205–1219.